Title
STRUCTURAL OBSERVATIONS IN A METASTABLE AUSTENITIC STEEL

Authors
Hall, James A.
Zackay, Victor F.
Parker, Earl R.

Publication Date
1969-04-01

Submitted to Transactions Quarterly of
American Society of Metals

UCRL-18770 Rev.
Preprint

c.2

STRUCTURAL OBSERVATIONS IN A METASTABLE AUSTENITIC STEEL

James A. Hall, Victor F. Zackay and Earl R. Parker

December 1969

AEC Contract No. W-7405-eng-48

LAWRENCE RADIATION LABORATORY
UNIVERSITY of CALIFORNIA BERKELEY

UCRL-18770 Rev.

DISCLAIMER

UCRL-18770 Rev

STRUCTURAL OBSERVATIONS IN A METASTABLE AUSTENITIC STEEL

James A. Hall, Victor F. Zackay and Earl R. Parker

Inorganic Materials Research Division, Lawrence Radiation Laboratory
Department of Materials Science and Engineering, College of Engineering,
University of California, Berkeley, California

ABSTRACT

The mechanical properties of a metastable austenitic steel (22.6Ni-4.02Mo-0.28C), after a thermomechanical treatment involving deformation at or above the A_s temperature, were determined. Yield points were present in the stress-strain curves of all specimens given a prior deformation of 20 percent or more. Both the volume fraction of martensite at fracture and the rate of work hardening varied with the angle to the rolling direction in sheet specimens. The morphologies of strain-induced and athermal martensite were observed to be similar when both types were produced from annealed austenite, but they were different when they were produced from deformed austenite.

INTRODUCTION

In order to obtain large amounts of elongation at any strength level, it is necessary to prevent the onset of plastic instability during tensile loading. The higher the yield strength, the greater must be the strain-hardening rate, $d\sigma/d\varepsilon$, if high values of elongation are to be realized. However, in quenched and tempered steels, the work-hardening rate ($d\sigma/d\varepsilon$) remains unchanged with increasing yield strength (1). Hence, in these steels, plastic instability begins at lower strains at the higher values of yield strength.

Several authors have recognized that certain phase transformations concurrent with straining will promote higher-work hardening rates and enhance the elongation. Hiltz (2) pointed out that in certain titanium alloys there occurs a strain-induced martensitic transformation which increases elongation. Bressanelli and Moskowitz (3) found a similar behavior with metastable austenitic stainless steels.

Until recently, these investigations and others have been limited to relatively low-strength materials. Zackay et al. (4) used this mechanism to promote elongation in high-strength metastable austenitic steels. They reported several compositions which exhibited a strain-induced martensite transformation in the austenite during tensile testing at room temperature. The authors suggested that the martensite provided barriers to dislocation motion stronger than dislocation tangles, thereby causing the work-hardening rate to increase and the onset of necking to be delayed.

The purpose of this investigation was to study the structure of one of the metastable steels during transformation in an attempt to gain a

better understanding of the relation between the transformation phenomenon and the mechanical properties. The steel chosen for the investigation contained 22.6 percent Ni, 4 percent Mo, and 0.28 percent C.

EXPERIMENTAL PROCEDURE

Melting and Rolling

The alloy was prepared by vacuum induction melting and cast in a copper mold. The resulting 20-lb. ingots were forged at 1100°C to plates 0.6 in x 3 in. in cross-section. Preliminary rolling was done at 900°C. This was followed by an austenitizing treatment of one hour at 1100°C and water quenching. The thermomechanical treatment was carried out by multipass rolling at 500°C, each reduction being 10 percent. After each pass through the rolls, the piece was reheated to 500°C. The strip was water quenched after the last pass. This elevated temperature treatment will be referred to hereafter as PDA (Prior Deformation of Austenite).

Mechanical Testing

A 0.010 in. layer was removed from each surface in order to eliminate the possible effects of surface decarburization or roll chill. The tensile specimens were flat and had a gage section 0.060 in. x 0.380 in. x 1.38 in. long. Samples were cut at 0°, 45°, and 90° with respect to the PDA rolling direction to check for anisotropy.

An Instron 100,000 lb. tensile machine was used at a crosshead speed of 0.04 in./min. Trial runs with crosshead speeds greater than this were found to cause reduction in ultimate tensile strengths because of specimen heating. Strain measurements were made with a one-inch extensometer capable of measuring strains up to 60 percent. The output of the extensometer was fed into the chart drive system of the Instron control console.

Optical Microscopy

Specimens were electropolished in a saturated solution of chromic oxide in phosphoric acid at a current density of 10 amperes per square inch and electroetched in the same solution. This method was used because mechanical polishing caused martensite to form. When necessary, a supplemental etch consisting of 5 grams cupric chloride in 100 cc each of water, hydrochloric acid and methyl alcohol was used.

Electron Microscopy

Thin foils were prepared by an initial light mechanical grinding from 0.060 in. to about 0.040 in., followed by chemical polishing to a thickness of about 0.005 in. in a 50 percent solution of H_2O_2 in phosphoric acid. Final thinning was accomplished by electropolishing, using the window technique, in the same polishing solution used for optical metallography. The current density was about 10 amperes per square inch. A Siemens Elmiskop IA electron microscope operated at 100 kV was used for the transmission microscopy.

Differential Thermal Analysis

The differential thermal analysis measurements were made by comparing the specimen with a nickel standard. Both of the 0.4 in. x 0.4 in. x 0.030 in. pieces were spot welded to iron-constantan thermocouples. They were heated in an argon atmosphere. The temperature of the nickel specimen and the difference between the two were recorded simultaneously. When the reversion of the martensite to austenite occurred, a sudden change in the differential temperature was recorded. This was taken to be the A_s (austenite start) temperature.

Electron Microprobe Analysis

A step trace measuring Mo L_α radiation was made on metallographic specimens. The L_α line was used, rather than K_α or K_β, because the latter two wavelengths are so short that the analyzing detector could not be positioned at an angle low enough for efficient detection. Quantitative measurements were not possible because the minimum electron beam spot size was larger than the average precipitate size. Therefore, only the Mo L_α intensity, in terms of counts per 10 second period, was measured and plotted.

Distribution of Martensite in Tensile Samples

After a tensile extension of 15%, successive layers of material were removed from the surface of the specimen by electropolishing. Several micrographs (magnification of 400x) were taken at each depth below the surface.

To measure the volume percent martensite at each level, a grid intercept-point count method was used (5). At least six 4 x 5 in. micrographs, divided into 2000 grid intersections, were used in obtaining each value.

Magnetic Measurements

Tensile specimens were cut 3/8 in. back from each side of the fracture and both pieces were measured for magnetic saturization (6). The volume percent of martensite present in fractured specimens was measured as a function of specimen orientation and of the amount of prior deformation. A magnetic correction for alloy content was made according to the data of Kittel (7).

EXPERIMENTAL RESULTS AND DISCUSSION

Tensile

Room temperature stress-strain curves are shown in Figs. 1 and 2. These curves show the effects of the thermo-mechanical deformation and of the specimen orientation (with respect to the PDA rolling direction). All specimens were austenitic prior to testing, but after testing the gage sections were strongly magnetic. By checking with a hand magnet during tensile testing it was found that martensite began to form at the onset of plastic straining, but the first martensite to form was more difficult to detect in specimens that did not exhibit the yield point phenomenon. The stress at which the strain induced martensite formed was increased by larger amounts of prior deformation at 500°C, as Fig. 1 shows.

Effect of Deformation and Orientation

Increased amounts of PDA resulted in higher yield and tensile strengths. Both the yield and tensile strengths varied slightly with the angle of the sheet specimen to the rolling direction. The results are summarized in Fig. 3. The total elongations to failure decreased with up to about 25% PDA and then began to increase with further PDA, as shown in Fig. 4. The total elongation also appears to be influenced somewhat by the orientation. The effect of orientation on the percent of martensite formed is shown in Fig. 5. The reason for this behavior is not known.

The rate of work hardening was strongly influenced by the amount of PDA. The work hardening exponent "n" in the true-stress true-strain relationship first increased with amount of PDA, then decreased as shown in Fig. 6. The work hardening rate, $d\sigma/d\varepsilon$, at particular strains, varied with the amount of PDA in much the same manner as the value of "n".

Figure 7 shows the effects of deformation and orientation on the work hardening rate at $\varepsilon = 0.15$. Similar curves were found at strain of 0.20 and 0.25. The assumption of the $\sigma = k\varepsilon^n$ relationship was well borne out for that part of the stress-strain curve between the end of the yield point strain and the maximum load. The end of the yield point strain (about 10 percent) corresponded to the formation of a volume fraction of martensite of about 35 percent for all room temperature tests. (However, other unpublished data obtained in the author's laboratory from tests conducted at both lower and higher temperatures indicated that there is no constant relationship between the yield point strain and the volume fraction of martensite formed during the straining.)

When PDA was 20 or more percent, the material had a yield point and a substantial amount of strain at the lower yield point stress. Fig. 8 shows photographs of a tensile specimen during the passage of a Luders' band along the specimen. The material inside the Luders' band strongly attracted a hand magnet while that outside did not, demonstrating that the Luders' band front separates the transformed and untransformed regions.

The total amount of martensite formed at 15 percent strain in specimens of the same orientation varied little with the amount of prior deformation.

Detail In the Stress-Strain Curves

All of the stress-strain curves had superimposed upon them numerous serrations consisting of rapid load drops followed by short periods of high work hardening rates. These serrations were not detected in the lower yield point strain region, nor were they detected below about 9 percent on the stress-strain curves of the material which showed no yield points. The magnitude of the load drops in the serrations increased

as the stress increased, reaching a maximum after the onset of necking.

Effect of Transforming the Martensite Prior to Testing

A specimen with 10 percent PDA was transformed by immersion in liquid nitrogen. This treatment increased in room temperature yield strength from 87 to 186 ksi and in tensile strength from 126 to 200 ksi. The total elongation decreased from 54 percent to 11.5 percent.

Microscopy After Thermomechanical Treatment, Prior to Room Temperature Testing

All the PDA material, when examined in cross section, exhibited a "banded" microstructure: the "banding" was more severe with higher amounts of PDA. Fig. 9 shows a cross-section view of a typically banded microstructure. An electron microprobe step-scan trace across bands of precipitated particles gave high peaks in the measured molybdenum L_α radiation. The trace is shown in Fig. 10. Transmission electron diffraction in a thin foil carefully prepared to retain the precipitates revealed them to be Mo_2C. An indexed electron diffraction pattern is shown in Fig. 11c. Figs. 11a and 11b show bright and dark filled micrographs of the area. Two precipitated particles were included in the selected area. They produced the two HCP diffraction patterns superimposed on the pattern for the FCC matrix. One diffraction spot from each HCP pattern was included in the aperture when taking the dark field micrograph.

The undeformed material, when examined metallographically, was found to contain no precipitates although it did seem to be segregated. When quenched to just below its M_s temperature, martensite formed in bands, as shown in Fig. 12.

Transmission microscopy revealed an increase in dislocation density with increasing amounts of PDA. There was a "cellular" type substructure in the 10 percent PDA material. The 20 percent and 30 percent PDA material contained more nearly uniform tangles and showed fewer cellular dislocation arrays. Figures 13a, b, and c are transmission micrographs for 0, 10, and 30 percent deformed material, respectively.

Observations Made After Room Temperature Tensile Tests

The general morphology of the strain-induced martensite does not vary much in appearance with the amount of prior deformation. Figures 14b and 14c are representative of the morphology of the strain-induced martensite found after 15 percent strain at room temperature on 10 percent and 20 percent PDA material. The same morphology of strain-induced martensite was observed in the material receiving 30 percent prior deformation. The morphology of the strain-induced martensite in the material having had no prior deformation is somewhat different, as shown in Fig. 14a.

In transmission electron microscopy, the strain-induced martensite appeared to be free of internal twinning, but it contained very dense dislocation networks. Examples of this are seen in Fig. 15. The electron diffraction patterns and micrographs gave no indication of twinning or precipitation outside of the banded areas mentioned previously.

In the material receiving no PDA, when strained to 5 percent elongation at room temperature, the resulting surface contain sharp needle-like upheavals while those appearing in the Luders' band show larger markings. Figure 16 shows the prepolished surface of the material (with no PDA) after room temperature straining. In this specimen, the removal of just

0.003 in. from the surface completely eliminated all evidence of martensite. Tensile samples of the material that received 10, 20, and 30 percent prior deformation, when strained at room temperature to 15 percent elongation (commensurate with passage of the Luders' bands), all showed a variation in volume percent martensite with distance from the surface. Figure 17 shows this dependence. Such dependence was present in all the materials examined and seemed to be most pronounced in the material with the least prior deformation.

Comparison With Athermal Martensite

The general microstructure of the strain-induced martensite was compared with that obtained by immersion in liquid nitrogen. The morphology of the strain-induced martensite, shown in Fig. 14, was not significantly altered by the amount of the PDA, as mentioned previously. However, the athermal martensite morphology varied, depending on the amount of PDA. Figures 18a through 18e show the microstructures obtained on quenching in liquid nitrogen. The morphology of strain-induced martensite in an austenite having no PDA is most nearly like that obtained in some regions of the athermally transformed previously undeformed material. (Compare 14a with 18a.) The morphology of strain-induced martensite in an austenite having been given prior deformation is distinctly different from that of athermal martensite produced by quenching a deformed austenite. (Compare 14b with 18b through 18e.)

SUMMARY

The mechanical properties of a metastable austenitic steel, (22.6Ni-4.02Mo-0.28C), after a thermomechanical treatment involving deformation at or above the A_s temperature, were measured.

The stress-strain curves of this steel exhibited a yield point when the prior deformation during the thermomechanical treatment was 20 percent or higher.

A change in the slope of the $\log_e \sigma$< vs $\log_e \varepsilon$ curves was observed for all steels, regardless of the amount of prior deformation, at a strain corresponding to a martensite content of about 35 percent. Beyond these strains, the curves were straight lines. The value of the work hardening coefficients obtained varied from 0.44 to 0.67. Serrations were observed in the work hardening portions of the stress-strain curves. Both the rate of work hardening and the volume fraction of martensite were observed to vary with the angle to the rolling direction in sheet specimens.

The morphologies of strain-induced and athermal martensite are observed to be similar when both types are produced from annealed austenite, but they were different when they are produced from deformed austenite.

ACKNOWLEDGEMENTS

The authors wish to express their appreciation to Professor G. Thomas for his advice and help. Thanks also are due to Dr. Dan Merz and Mr. W. W. Gerberich for their many helpful discussions and support.

This work was performed under the auspices of the United States Atomic Energy Commission through the Inorganic Materials Research Division of the Lawrence Radiation Laboratory.

REFERENCES

1. F. R. Larson, and J. Nunes, Trans. ASM, 53 (1966) 663.

2. R. Hiltz, Trans. AIME, 215 (1959) 138.

3. J. Bressanelli and A. Moskowitz, Trans. ASM, 59 (1966) 223.

4. V. F. Zackay, E. R. Parker, D. Fahr, and R. Busch, Trans. ASM, 60 (1967) 252.

5. W. Rostoker and J. R. Dvorak in Interpretation of Metallographic Structure, Academic Press, New York (1965) 198.

6. B. DeMiramon, (M. S. Thesis), University of California, Sept. (1967).

7. C. Kittel, Ed., in Introduction to Solid State Physics, 3rd Ed., John Wiley and Sons, New York, (1967) 470.

8. F. A. McClintock and A. S. Argon, in Mechanical Behavior of Materials, Addison-Wesley, Reading, Mass., (1966) 321.

LIST OF FIGURES

Fig. 7 Work hardening rate "$d\sigma/d\varepsilon$" in room temperature tensile test for various orientations as a function of amount of deformation at 500°C. $d\sigma/d\varepsilon$ determined at $\varepsilon = 0.15$.

Fig. 8 a-d Tensile sample which had been prepolished and then strained 3.5 percent at room temperature. The material had received 30 percent deformation by rolling at 500°C. The tensile axis was parallel to the rolling direction. Luder's bands visible at top in (a). Note the occurrence of considerable plastic deformation outside the "Luder's" band. At this stage the area inside the "Luder's" band was strongly attracted by a hand magnet while that outside was not. Magnifications indicated on pictures in (b), (c) and (d).

Fig. 9 Cross section of material after 30 percent deformation at 500°C. Note the heavily banded microstructure. In some areas, slip bands are visible even after repolishing and re-etching, indicating that there were some very small precipitates decorating the slip bands. Magnification indicated on photomicrograph.

Fig. 10 Electron microprobe step trace across some of the banded microstructure of Fig. 9. Mo L_α was measured in counts per 10 sec. Similar measurements for iron and nickel failed to show any significant variations as the trace crossed the bands of precipitated particles.

Fig. 11 (a) Bright field transmission electron micrograph showing some of the larger precipitates in the bands of the microstructure. (b) Dark field micrograph utilizing the two diffraction spots indicated. Note that the two precipitates are light. (c) Selected area diffraction pattern containing both of the two precipitated particles which reversed contrast in the dark field. Two HCP diffraction patterns of Mo_2C are superimposed on the FCC matrix. As indexed, both precipitates are of the $\langle 12\bar{3} \rangle_{Mo_2C}$ orientation while the matrix is of a $\langle 110 \rangle_n$ orientation.

Fig. 12 Optical micrograph of austenitized material with no deformation quenched to a temperature just below the M_s. Note how the martensite forms in parallel bands.

Fig. 13 Transmission electron micrographs of the material with various thermomechanical treatments.

(a) Austenitized and held with no deformation at 500°C.

(b) Austenitized with 10 percent deformation at 500°C. Note cellular dislocation substructure.

(c) Austenitized with 30 percent deformation at 500°C. Note the almost complete absence of a cellular substructure.

Fig. 14 Micrographs of strain-induced martensite. Magnification marked on photomicrographs.

(a) In necked region of the tensile specimen having had no deformation at 500°C. Tensile tests at room temperature.

(b) In material having had 10 percent deformation at 500°C and then strained 15 percent at room temperature.

(c) In material having had 20 percent deformation at 500°C and then strained 15 percent at room temperature.

Fig. 15 Representative transmission electron micrographs of strain-induced martensite taken from two areas in the specimen. The material had 20 percent deformation at 500°C followed by 30 percent elongation in tension at room temperature. There appears to be no twinning or observable precipitation (except the large particles carried over from the banded austenite as shown in Fig. 11).

Fig. 16 A photomicrograph of a polished tensile specimen strained 5 percent in tension at room temperature. This material had received no prior deformation at 500°C.

Fig. 17 Variations of amount of martensite with distance from surface of three tensile specimens strained 15 percent at room temperature. One was deformed 10 percent at 500°C, the second one 20 percent, and the third one 30 percent.

Fig. 18 Microstructures of athermally formed martensite obtained by cooling to -196°C in liquid nitrogen.

(a) Material with no prior deformation at 500°C.

(b) Material with 10 percent prior deformation at 500°C.

(c) Material with 30 percent prior deformation at 500°C.

(d) Material with 20 percent prior deformation at 500°C, face of rolled strip.

(e) Material with 20 percent prior deformation at 500°C, edge cross section of rolled strip.

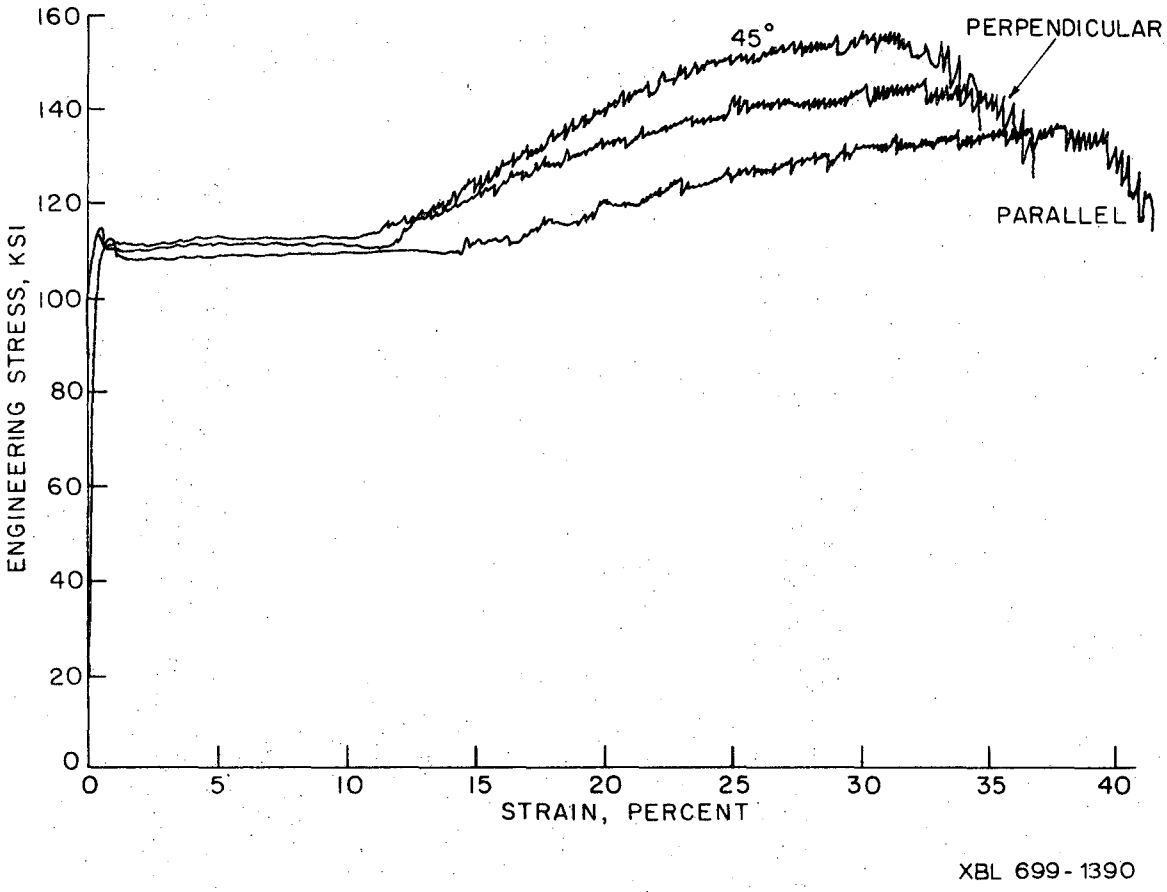
160
140
120
100
80
60
40
20
0
ENGINEERING STRESS, KSI
45°
PERPENDICULAR
PARALLEL
0
5
10
15
20
25
30
35
40
STRAIN, PERCENT
XBL 699-1390

Fig. 1

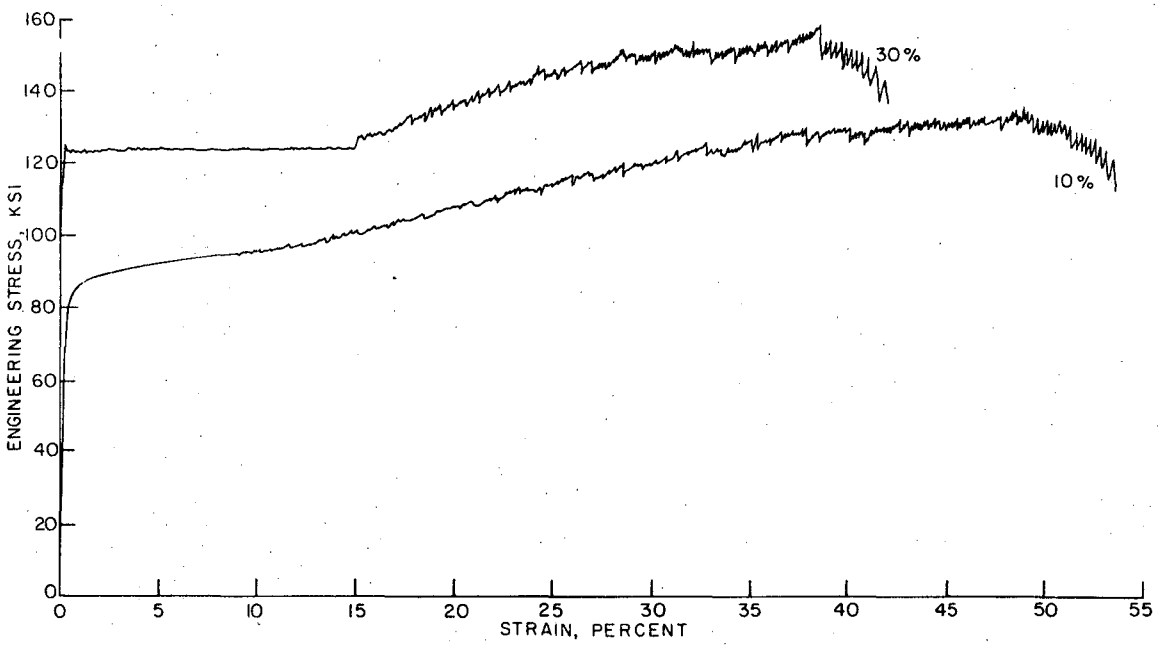

XBL 699-1389

Fig. 2

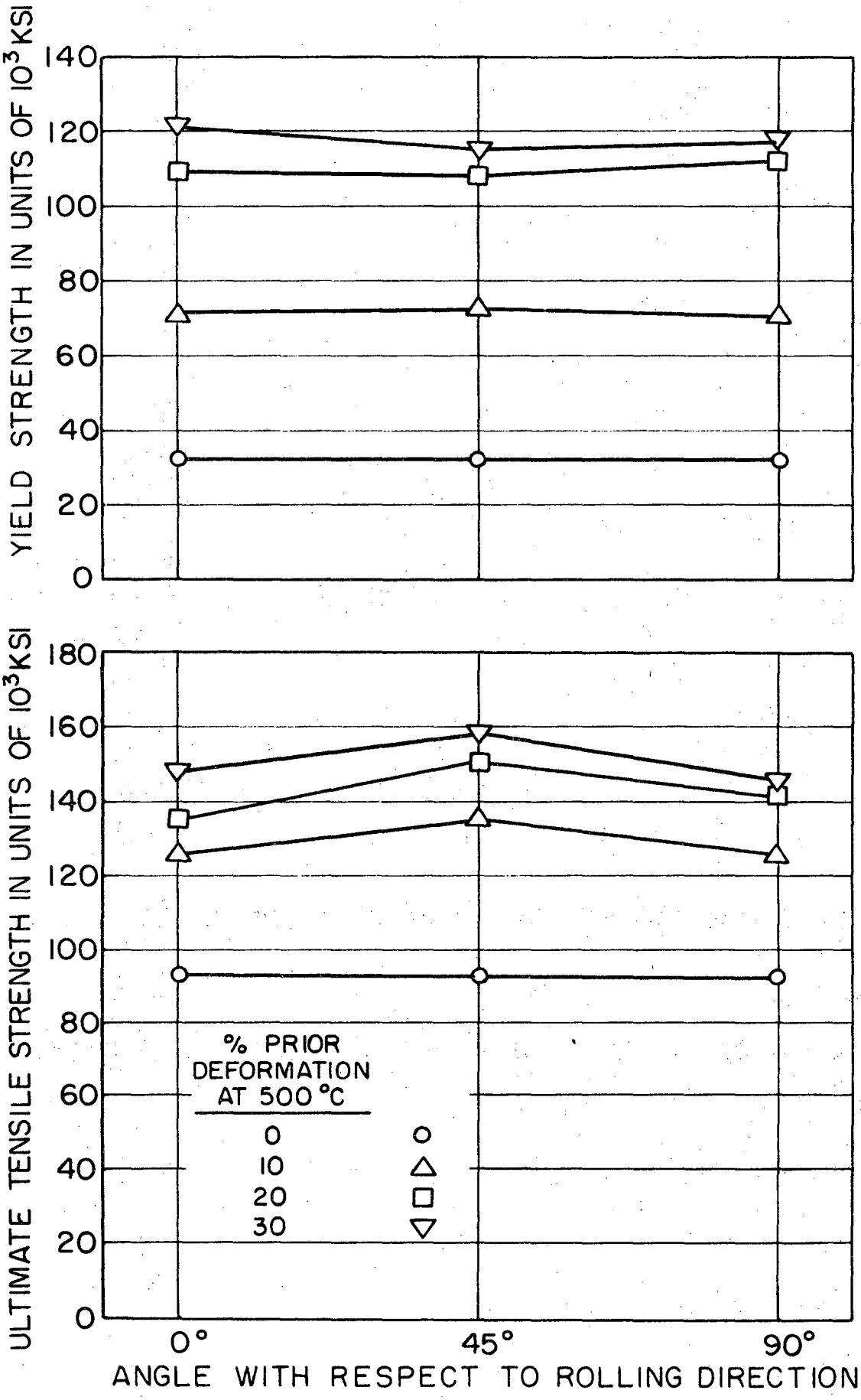

Fig. 3

XBL 685-740

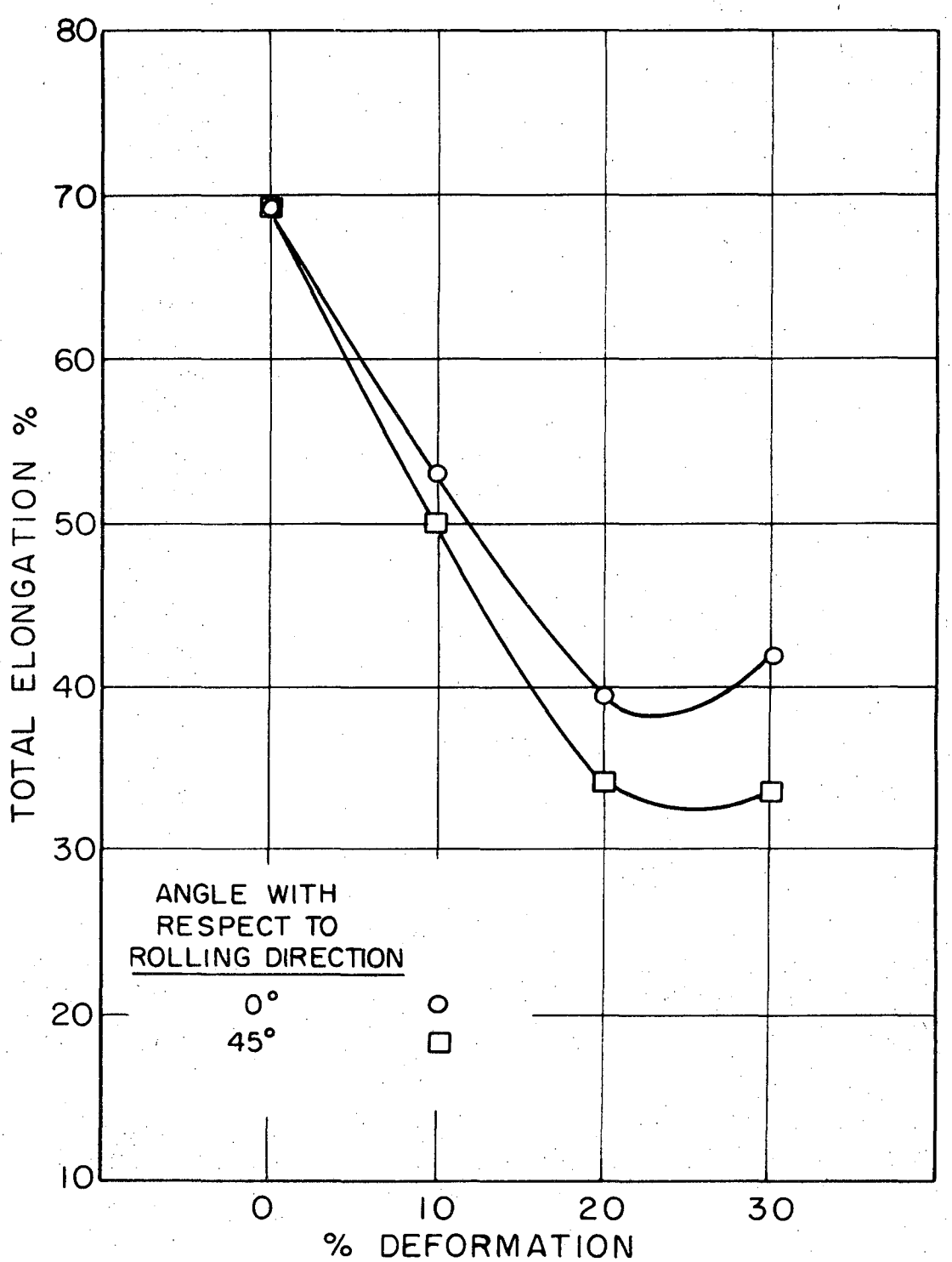

XBL 685-746-A

Fig. 4

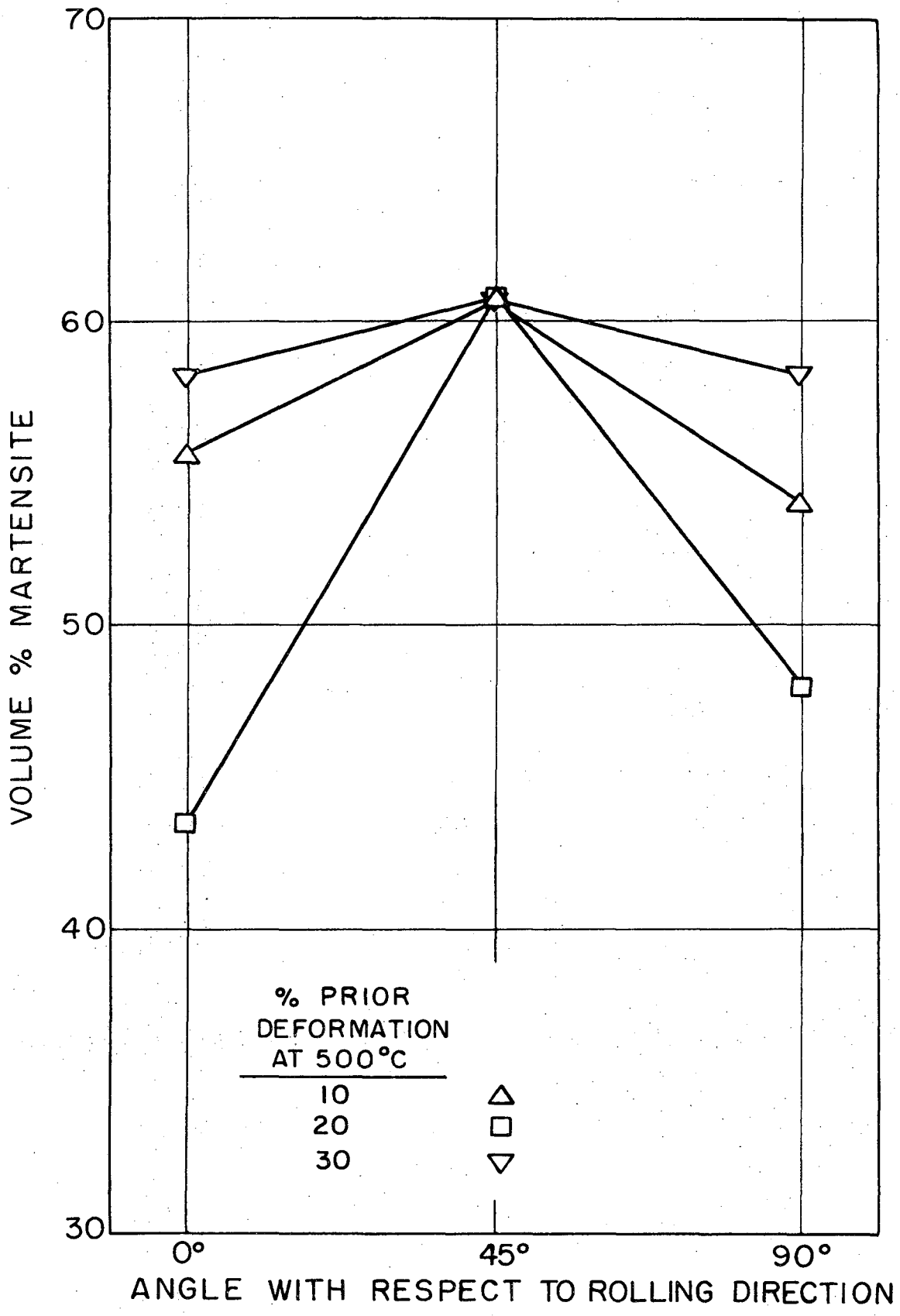

XBL 685-746-B

Fig. 5

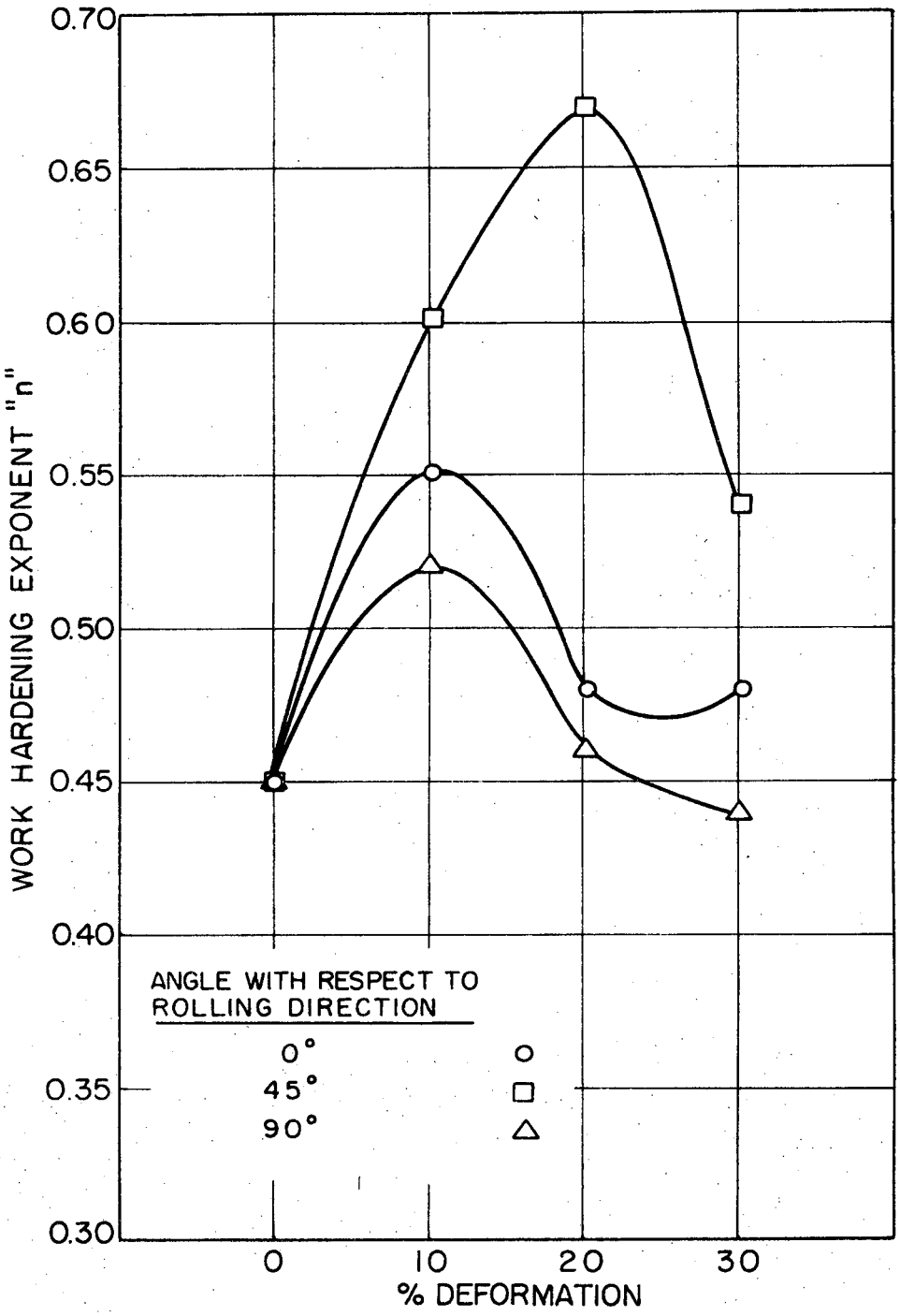

XBL 685-745-A

Fig. 6

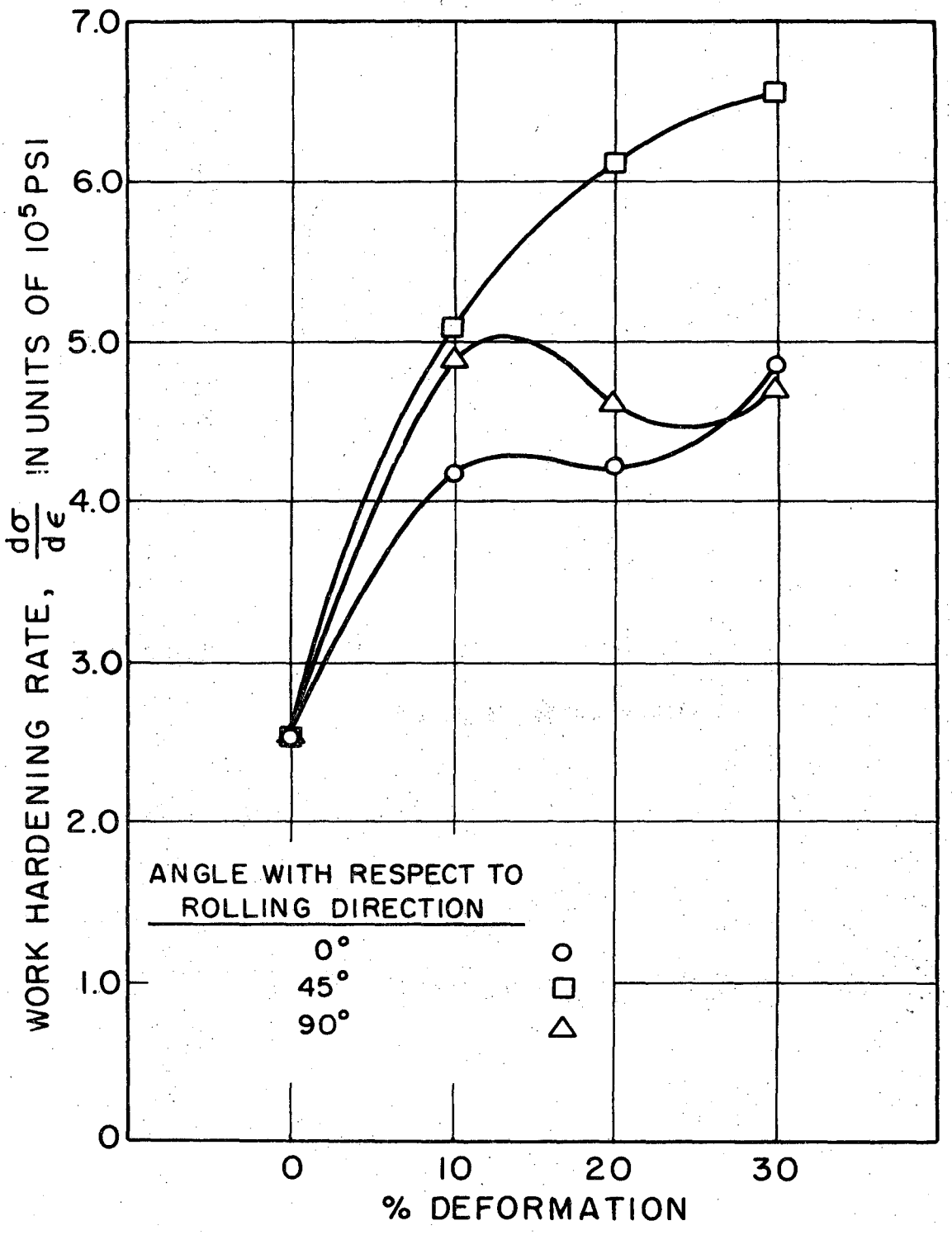

XBL 685-745-B

Fig. 7

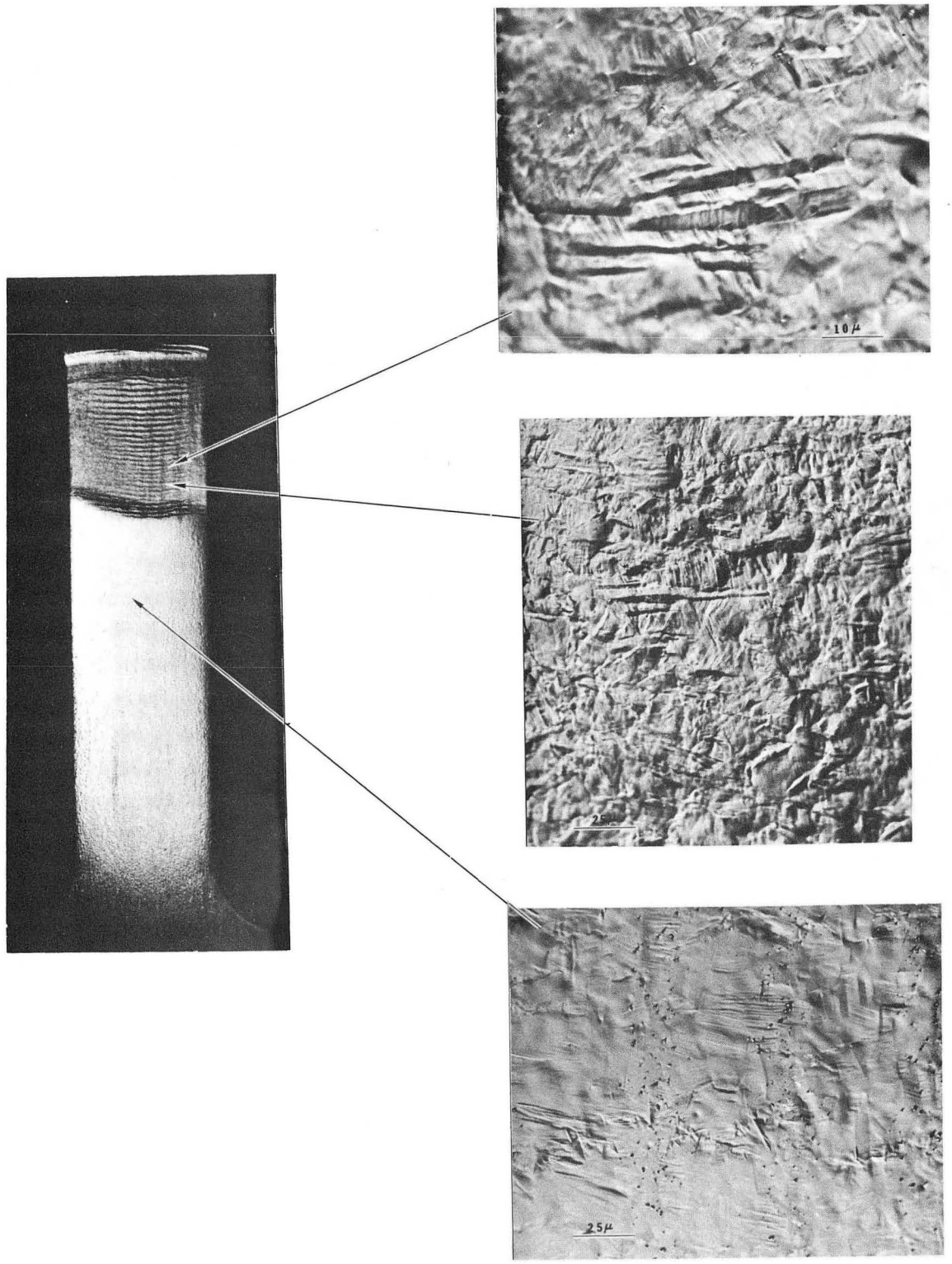

XBB 685-2820

Fig. 8

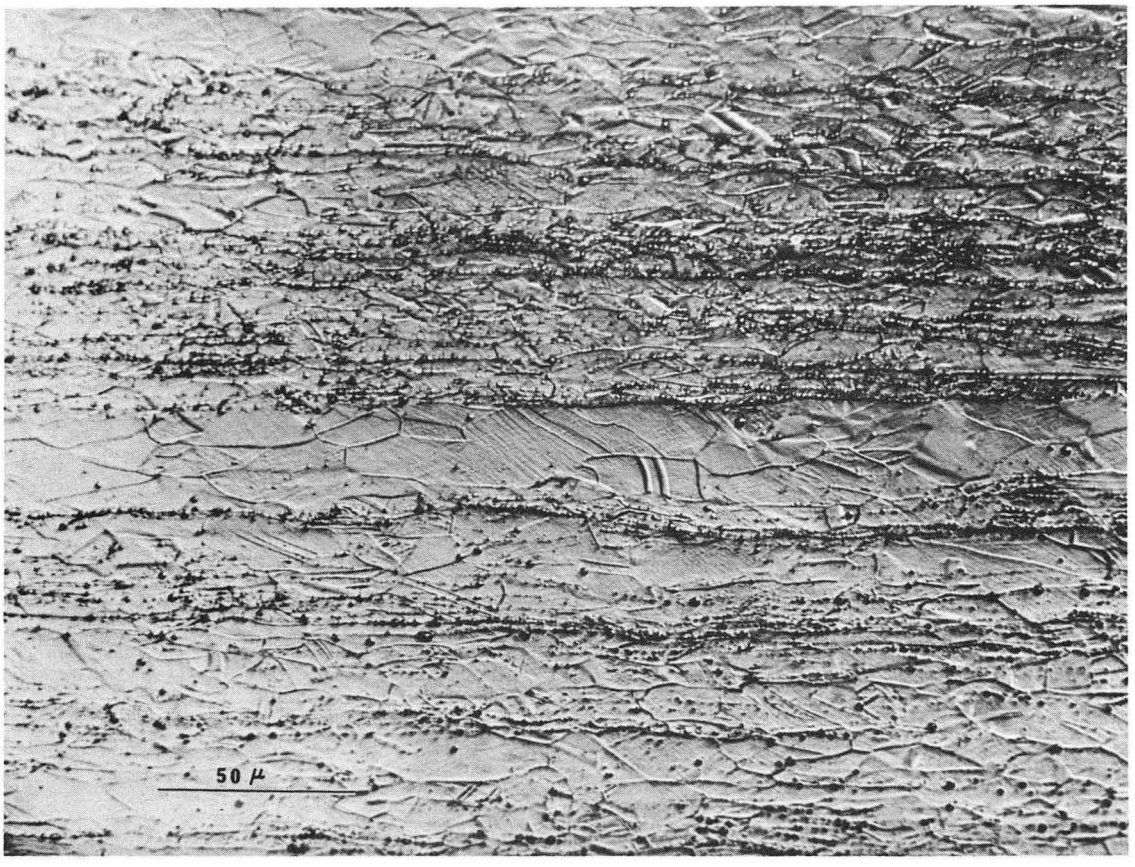

XBB 685-2814

Fig. 9

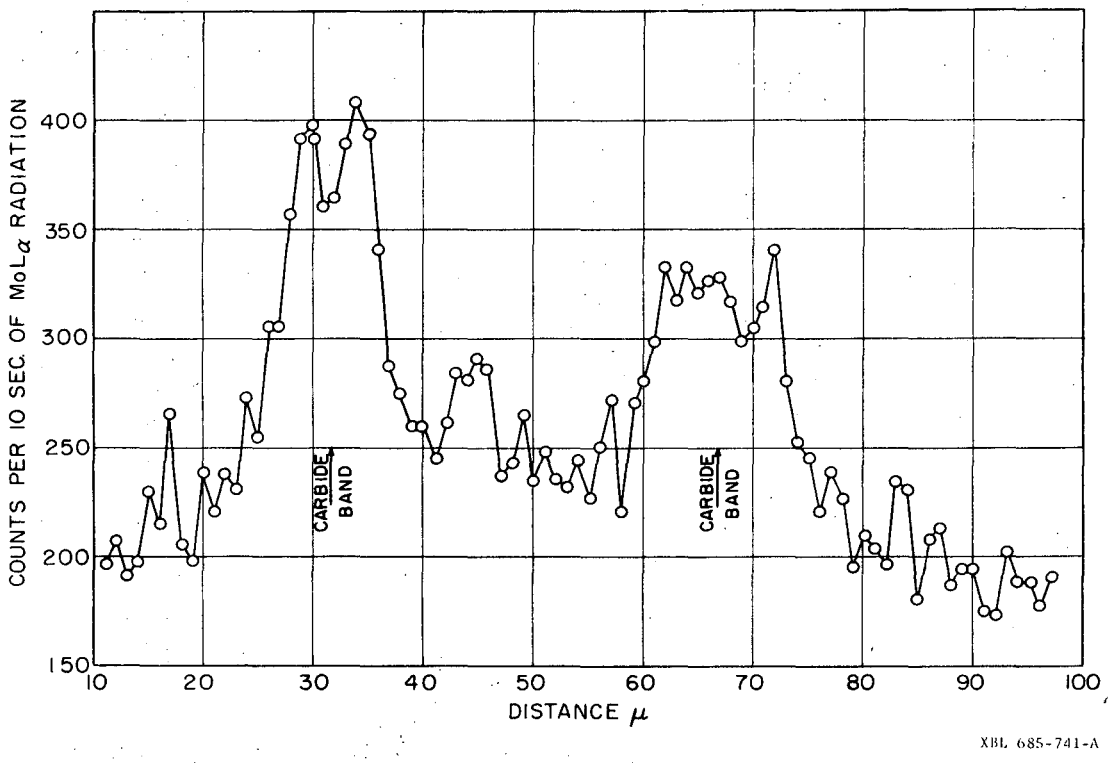
COUNTS PER 10 SEC. OF MoLα RADIATION
400
350
300
250
200
150
10
20
30
40
50
60
70
80
90
100
DISTANCE μ
CARBIDE BAND
CARBIDE BAND
XBL 685-741-A

Fig. 10

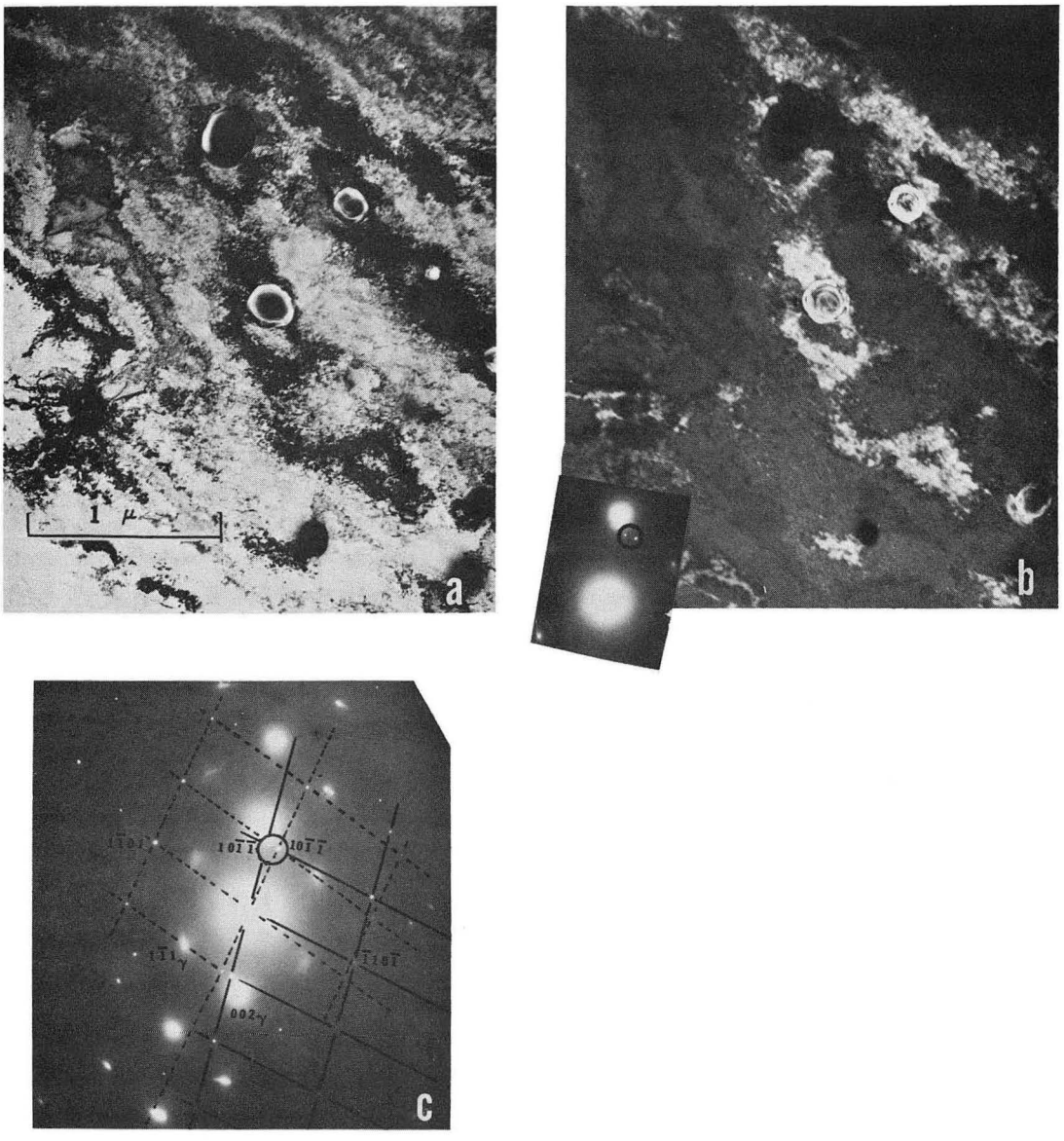

XBB 685-2816A

Fig. 11

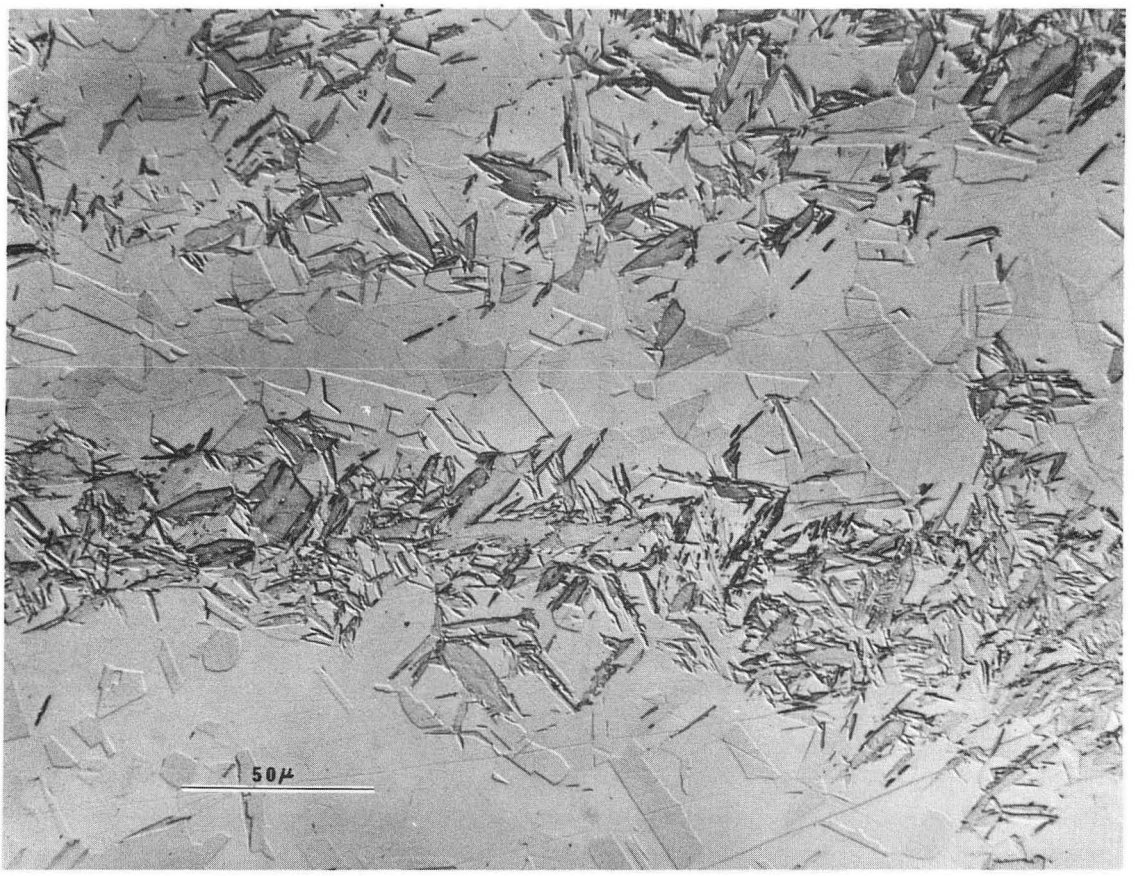

XBB 685-2813

Fig. 12

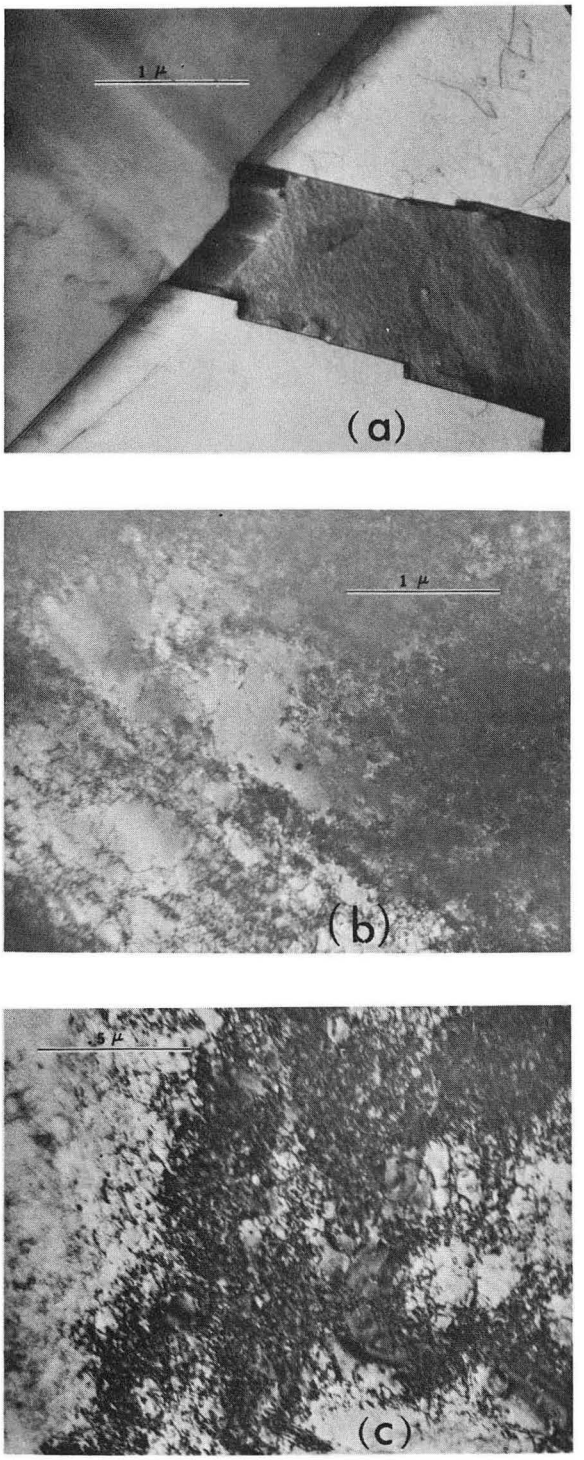

XBB 685-2819A

Fig. 13

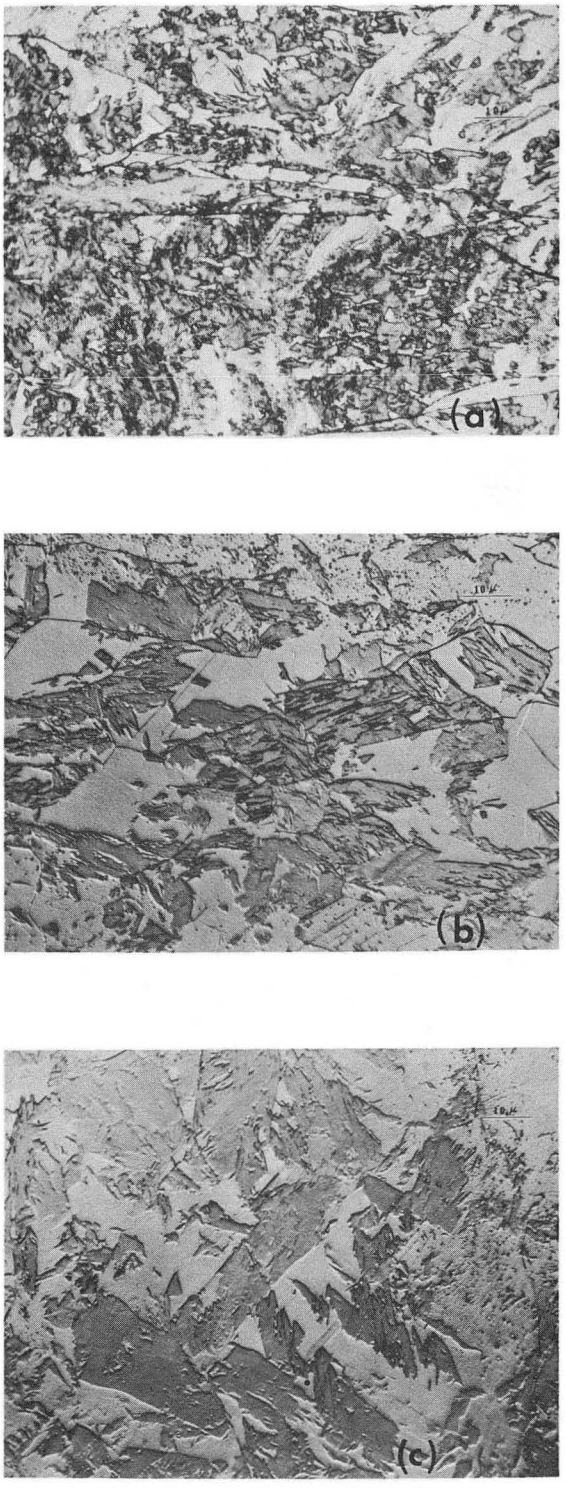

XBB 685-2815A

Fig. 14

XBB 685-2817

Fig. 15

XBB 685-2812

Fig. 16

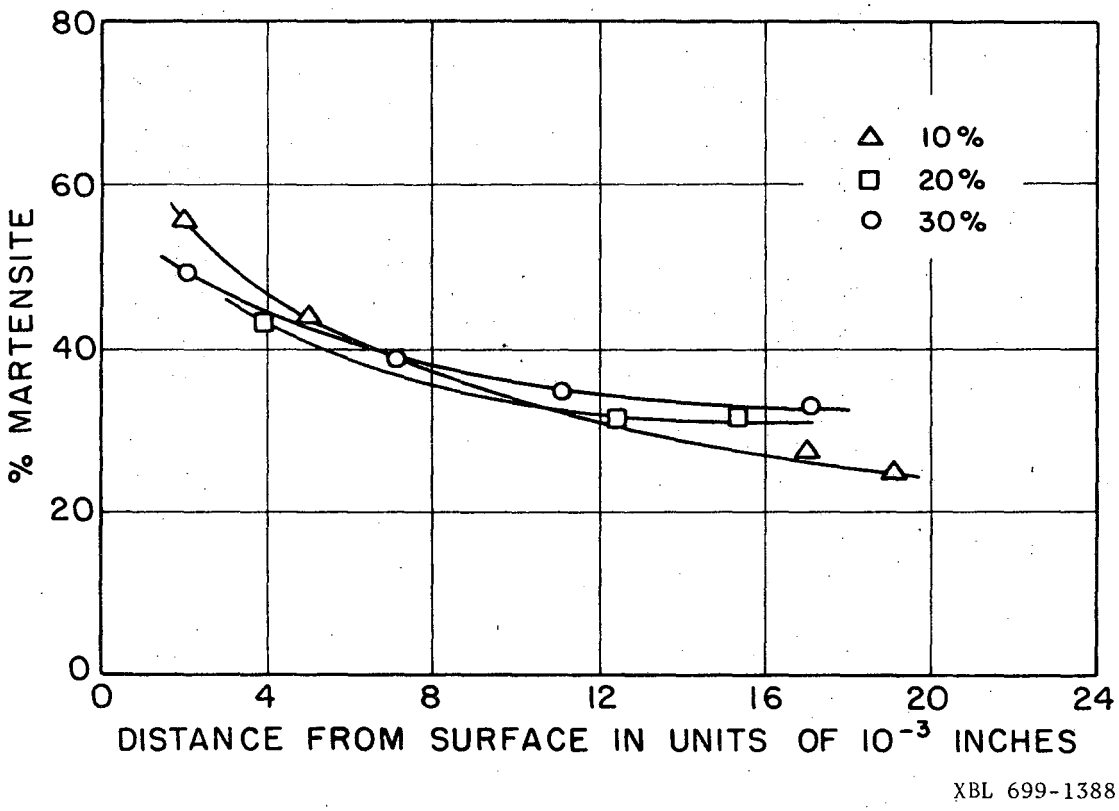
80
60
40
20
0
% MARTENSITE
0
4
8
12
16
20
24
DISTANCE FROM SURFACE IN UNITS OF 10^{-3} INCHES
10%
20%
30%
XBL 699-1388

Fig. 17

a

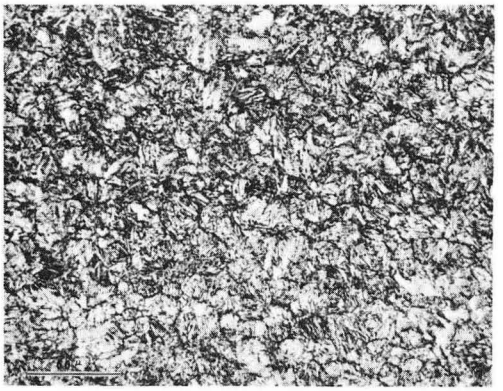

b

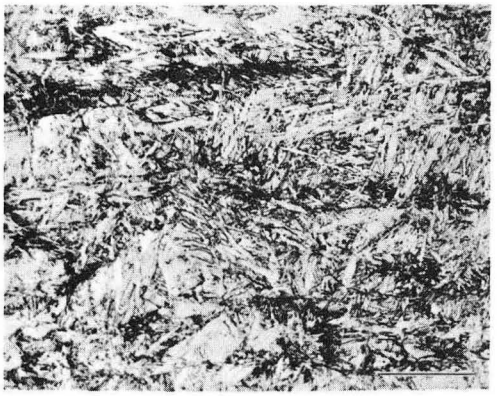

c

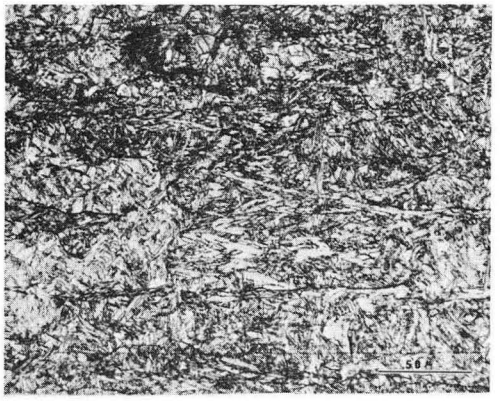

d

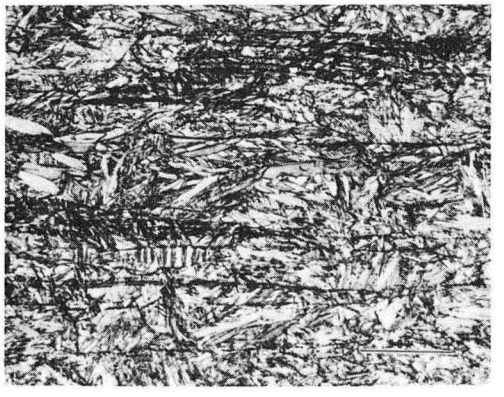

e

XBB 685-2818

Fig. 18

TECHNICAL INFORMATION DIVISION
LAWRENCE RADIATION LABORATORY
UNIVERSITY OF CALIFORNIA
BERKELEY, CALIFORNIA 94720